Chain Interactions in Poor-Solvent Polymer Solutions: Equilibrium and Nonequilibrium Aspects

Guido Raos and Giuseppe Allegra*

Dipartimento di Chimica, Politecnico di Milano, Via L. Mancinelli 7, 20131 Milano, Italy

Received April 3, 1996; Revised Manuscript Received July 3, 1996[⊗]

ABSTRACT: In this paper, we compute the interaction free energy between two polymer chains as a function of their separation R, in the poor-solvent regime below the ideal Θ temperature. We present both conventional "equilibrium" and "frozen-chain" nonequilibrium interaction free energies: in the latter case, the conformational state of the chains is not allowed to relax as they approach. The two types of calculation correspond to two distinct limits for the relative magnitudes of the "diffusion time" and the "conformational relaxation time" of the chains and give qualitatively different results below the collapse temperature. Both times scale as ηN, η being the solvent viscosity and N the chain length. Hence the true chain interaction free energy corresponds neither to the equilibrium nor to the frozen-chain one, but to some kind of interpolation of the two whose form remains to be examined. The role of the chain entanglements is also briefly discussed: their relaxation time scales as $\eta N^{7/3}\alpha_S^{-4}$, α_S being the contraction ratio of the chain radii of gyration over the unperturbed state. The second virial coefficient A_2 is computed from the cluster integral of the chain interaction free energy: below the collapse temperature, the equilibrium and the frozen-chain values of A_2 can differ by up to 3 orders of magnitude. We prove that a mean-field expression for A_2 derived by us in a previous paper is the first term in the series expansion of the frozen-chain coefficient. Finally, we discuss the implications of our findings for the shape of the polymer-solvent phase diagram and for the interpretation of Chu's experiments on the kinetics of chain collapse and aggregation.

I. Introduction

In a recent paper,[1] we proposed a unified description of the phenomena of chain collapse and of phase separation, which occur in a variety of polymer/solvent systems below the ideal Θ temperature.[2−4] This was made possible by our derivation of a mean-field expression for the free energy of the polymer solution as a function of the mean-square radius of gyration of the polymer chains $\langle s^2\rangle$, the polymer volume fraction φ, and the reduced temperature τ:

$$\tau = \frac{T-\Theta}{T} \qquad (\tau < 0 \text{ for } T < \Theta) \tag{1}$$

The polymer molecules were described by Gaussian chains, each consisting of N statistical segments ($N \gg 1$) of mean-square length l^2. The segments, belonging either to the same or to different polymer chains, were allowed to interact in pairs or triplets according to the effective potentials:

$$a_2(i,j) \propto \tau B l^3 \delta(r_{ij}), \qquad a_3(i,j,k) \propto K_1 l^6 \delta(r_{ij})\delta(r_{jk}) \qquad (B, K_1 > 0) \tag{2}$$

Notice that a_3 is independent of temperature, whereas a_2 is attractive for $T < \Theta$ and repulsive for $T > \Theta$.

Starting from our free energy expression, we obtained further useful information. By minimizing it with respect to the chain radius of gyration, we studied the temperature and concentration dependence of the chain dimensions. Let us indicate by α_S the expansion factor of the chain radius of gyration:

$$\alpha_S = [\langle s^2\rangle/\langle s^2\rangle_0]^{1/2} \tag{3}$$

where $\langle s^2\rangle_0$ is the radius of gyration of an "unperturbed" polymer chain, as in the melt or in the Θ solution:

$$\langle s^2\rangle_0 = \frac{1}{6} N l^2 \tag{4}$$

We found that for a given strength of the three-body repulsions, α_S is a single-valued universal function of all the remaining parameters:

$$\alpha_S(\tau,\varphi,N,B,K_1) = f_{K_1}[(\tau B + F K_1 \varphi) N^{1/2}] \tag{5}$$

where F is a system-dependent positive constant defined in ref 1. Our results on single-chain collapse ($\varphi = 0$) are shown in Figure 1 for two different systems, characterized by different values of the three-body parameter K_1. We identify the respective collapse

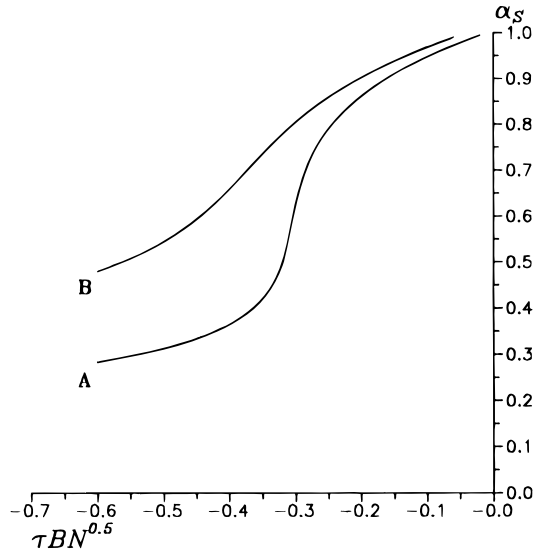

Figure 1. Contraction ratio for the single chains, α_S, as a function of $\tau BN^{1/2}$. The three-body parameters are $K_1 = 1.9 \times 10^{-3}$ for A and $K_1 = 7.6 \times 10^{-3}$ for B. The other system parameters, N and B, do not influence the shape of the plots.

* To whom correspondence should be addressed.

[⊗] Abstract published in *Advance ACS Abstracts,* September 1, 1996.

S0024-9297(96)00503-7 CCC: $12.00

temperatures with the inflection points of α_S, which occur at $\tau BN^{1/2} \simeq -0.30$ for A and at $\simeq -0.35$ for B. We also produced plots of the binodal and spinodal lines of the polymer/solvent phase diagram. The critical point of the phase separation transition is located above the collapse temperature, but their relative separation decreases as K_1 increases. Using $\varphi N^{1/2}$ and $(\tau - \tau_0)B(N/K_1)^{1/2}$ for the coordinate axes, with $\tau_0 = -16K_1/3BN^{1/2}$, we were able to superimpose on a single master curve the binodal lines for different polymer/solvent systems: we considered this result an empirical proof of a universal behavior of the coexistence curves. On the other hand, we also found that sufficiently far from the critical point, the spinodals do not share this interesting property. Thus, also the "observed" universality of the binodals is probably not exact, but only approximate.

As part of our mean-field analysis of the polymer solution, we obtained an explicit expression for the osmotic pressure and, by taking its second derivative with respect to the polymer concentration at $\varphi = 0$, for the second virial coefficient:

$$A_{2,\mathrm{mf}} \propto \tau B + \frac{3^{3/2}K_1}{N^{1/2}\alpha_S{}^3} \tag{6}$$

(the proportionality constant can be found in ref 1). We see that the mean-field A_2 is simply the sum of a two-body and of a conformation-dependent three-body term, where the chain expansion factor α_S is equal to that of the isolated chains at the same temperature. Below the Θ temperature, this function is almost everywhere negative, implying the existence of an effective attraction between the polymer chains. For the sake of precision, we point out that A_2 is actually positive at $\tau = 0$. Careful numerical analysis shows that it goes to zero and then to negative values only slightly below the Θ temperature, at $\tau \simeq \tau_0 < 0$ (recall that τ_0 has been introduced above in connection with the universality of the phase diagram). The reason for this Θ-temperature shift is simple: the two-body interactions operating between the monomers must be slightly attractive ($\tau B < 0$) in order to compensate for the three-body repulsions. However, the most striking feature of the mean-field A_2 is the presence of a minimum, which in general occurs just below the collapse temperature. The repulsive three-body interactions, which prevent collapse of the chain to a pointlike object, are also at the origin of the upturn in A_2. Consider eq 6: above the collapse temperature, α_S is relatively large and temperature-independent, so that the linear τB term dominates; at the collapse temperature, α_S decreases suddenly, thus causing a sharp increase of the positive contribution to A_2 and the appearance of the minimum.

The mean-field results on the second virial coefficient suggest an interpretation of the structure of the collapsed chains as compact objects, resisting mutual compenetration. Our purpose here is to verify this interpretation by alternative, more direct and transparent calculations of A_2. Thus, in sections II and III we address the following problems:

(a) the form of the interaction free energy between two chains in a poor solvent as a function of the separation between their centers of mass;

(b) the calculation of A_2 as cluster integral of the chain interaction energy defined above and its comparison with the mean-field approximation (6).

As we shall see, the shape of the interaction energy between two chains depends crucially on the relaxation of their internal degrees of freedom. In general, this relaxation can only occur over a finite amount of time. One is then led to consider the following issue:

(c) the influence of kinetic or nonequilibrium effects on the chain interaction free energy and the second virial coefficient. The importance of nonequilibrium effects in poor-solvent polymer solution has been stressed previously by Chu *et al.*[5] on the experimental side and by Grosberg and Kuznetsov[6] on the theoretical one.

The value of the second virial coefficient influences the shape of the polymer−solvent phase diagram. In particular, at the temperature where our mean-field A_2 goes through a minimum and then increases, the low-concentration branch of the spinodal in the calculated phase diagram stops approaching the $c = 0$ axis and turns to higher polymer concentrations.[1] To check this result, we address in section IV the last main point in the program of the paper:

(d) the implications of the results of points a−c above for the shape of the polymer−solvent phase diagram, including its near-universality observed in ref 1.

Finally, in section V we summarize our results and discuss their implications for the interpretation of the light scattering experiments on polymer collapse and aggregation by Chu and co-workers.[5]

II. Chain Interaction Free Energy

In this section, we present the theoretical framework and a series of numerical results for the interaction free energy between two polymer chains in a poor solvent. This problem has been tackled before by Tanaka[7] and by Grosberg and Kuznetsov[8] using different theoretical approaches. The general level of the theory adopted here is strictly comparable to that of our previous paper,[1] so that the reader can refer to it for further details.

Theory. In the present formulation, the energy of two interacting linear chains is a function of their separation R and of their mean-square radii of gyration $\langle s_1{}^2\rangle$ and $\langle s_2{}^2\rangle$ (N, B, K_1, and τ are of course other parameters of the problem). It can be decomposed into three distinct contributions[9,10] (energies are measured in k_BT units throughout):

$$A_{12}(R,\langle s_1{}^2\rangle,\langle s_2{}^2\rangle) = A_{\mathrm{cont}}(R,\langle s_1{}^2\rangle,\langle s_2{}^2\rangle) + A_{\mathrm{el},1}(\langle s_1{}^2\rangle) + A_{\mathrm{el},2}(\langle s_2{}^2\rangle) \tag{7}$$

The first term in eq 7 represents the contact free energy among the monomers belonging either to the same or to different chains. The second and third terms represent the conformational entropy of two chains whose average overall sizes are specified by $\langle s_1{}^2\rangle$ and $\langle s_2{}^2\rangle$, respectively. The "el" subscript stands for "elastic", since it is this particular type of free energy which provides the mechanism for rubber elasticity. The following paragraphs are devoted to the precise definition of all these quantities.

Let us consider two polymer chains whose centers of mass are located at points $\mathbf{R}_1$ and $\mathbf{R}_2$. It has been shown previously[11] that the average monomer density of an isolated polymer chain in a poor solvent ($T < \Theta$, $\alpha_S < 1$) is fairly well described by a simple Gaussian distribu-

tion. We assume that this is also true when the chains are at a finite distance $R = |\mathbf{R}_1 - \mathbf{R}_2|$:

$$\rho_i(\mathbf{r}) = \rho(|\mathbf{r}-\mathbf{R}_i|,\langle s_i^2\rangle) = N\left(\frac{2}{3}\pi\langle s_i^2\rangle\right)^{-3/2} \exp\left\{-\frac{3}{2}\frac{(\mathbf{r}-\mathbf{R}_i)^2}{\langle s_i^2\rangle}\right\}, \qquad (i = 1, 2) \quad (8)$$

The treatment could be made slightly more general by assuming anisotropic Gaussian distributions, with different amplitudes along the interchain axis and perpendicularly to it.

The energy of the contacts among the chain segments is the sum of two- and three-body contributions:

$$A_{\mathrm{cont}}(R,\langle s_1^2\rangle,\langle s_2^2\rangle) = A_2(R,\langle s_1^2\rangle,\langle s_2^2\rangle) + A_3(\mathrm{R},\langle s_1^2\rangle, \langle s_2^2\rangle) \quad (9)$$

Starting from eqs 2 and 8, their expressions can be shown to be given by (ref 1 contains the derivation in the special case $\langle s_1^2\rangle = \langle s_2^2\rangle$):

$$\frac{A_2}{\tau B N^{1/2}} = 2^{-5/2}\left(\frac{\langle s_1^2\rangle}{Nl^2}\right)^{-3/2} + 2^{-5/2}\left(\frac{\langle s_2^2\rangle}{Nl^2}\right)^{-3/2} + \left(\frac{\langle s_1^2\rangle + \langle s_2^2\rangle}{Nl^2}\right)^{-3/2} \exp\left\{-\frac{3}{2}\frac{R^2}{\langle s_1^2\rangle + \langle s_2^2\rangle}\right\} \quad (10)$$

$$\frac{A_3}{K_1} = \frac{1}{2\times 3^{5/2}}\left(\frac{\langle s_1^2\rangle}{Nl^2}\right)^{-3} + \frac{1}{2\times 3^{5/2}}\left(\frac{\langle s_2^2\rangle}{Nl^2}\right)^{-3} + \frac{1}{2}\left(\frac{\langle s_1^2\rangle}{Nl^2}\right)^{-3/2}\left(\frac{\langle s_1^2\rangle + 2\langle s_2^2\rangle}{Nl^2}\right)^{-3/2} \exp\left\{-3\frac{R^2}{\langle s_1^2\rangle + 2\langle s_2^2\rangle}\right\} + \frac{1}{2}\left(\frac{\langle s_2^2\rangle}{Nl^2}\right)^{-3/2}\left(\frac{\langle s_2^2\rangle + 2\langle s_1^2\rangle}{Nl^2}\right)^{-3/2} \exp\left\{-3\frac{R^2}{\langle s_2^2\rangle + 2\langle s_1^2\rangle}\right\} \quad (11)$$

The first and the second terms in eq 10 describe *intra*chain 1−1 and 2−2 contacts, whereas the third term accounts for *inter*chain 1−2 contacts; similarly, eq 11 consists of four terms, which correspond to 1−1−1, 2−2−2, 1−1−2, and 1−2−2 contacts, respectively.

The elastic free energy of each chain is a function of a "compression parameter" q_i, which also specifies the degree of chain contraction:[1,12,13]

$$A_{\mathrm{el},i} = \frac{3}{2}\left[\ln\left(\frac{\sinh q_i}{q_i}\right) - q_i \coth q_i + \frac{1}{2}\right] \quad (12)$$

$$\alpha_{s,i} = \left[\frac{1}{12 q_i}\left(\coth q_i - \frac{1}{q_i}\right)\right]^{1/2} \quad (13)$$

We shall limit our attention to positive values of q_i: $q_i \to 0^+$ describes the unperturbed state whereas $q_i \to +\infty$ represents the limit of strong chain collapse. Notice that $\alpha_{S,i}$ is a strictly decreasing function of q_i. Thus one could *in principle* invert eq 13, substitute the result into eq 12, and obtain a direct expression for the dependence of the elastic energy on the radius of gyration. Unfortunately, this inversion cannot be done in terms of ordinary analytical functions, so that one is obliged to use the auxiliary variable q_i and consequently both of eqs 12 and 13. This is not a serious disadvantage since these expressions can be easily handled numerically.[1]

The reason for adopting this slightly involved definition of the elastic free energy is that—unlike simpler ones which have appeared in the literature (see ref 14 for a critical review)—it can be derived from the exact expression for the conformational entropy of a Gaussian chain under the following assumptions: (a) the contact free energy A_{cont} is a single-valued function of the chain radius of gyration and (b) intramolecular entanglements do not limit or constrain appreciably the conformations accessible to the polymer molecule (phantom chain model). Assumption (a) is well justified in poor-solvent conditions[11] and indeed our single-chain contact free energy depends only on the radius of gyration (see eqs 9−11 for $R \to \infty$). As to the chain entanglements, they have an important influence on the chain dynamics but do not affect the equilibrium properties. We briefly return to this matter below.

All the equilibrium properties of the interacting chains follow from the partition function of the system. In particular, the interaction free energy as a function of *R only* is given by

$$A_{12}(R) = -\ln Z(R) \quad (14)$$

which in the present case is given simply by

$$Z(R) = \int_0^\infty \mathrm{d}\langle s_1^2\rangle \int_0^\infty \mathrm{d}\langle s_2^2\rangle \exp\{-A_{12}(R,\langle s_1^2\rangle,\langle s_2^2\rangle)\} \quad (15)$$

Here however we adopt a simpler variational approach, which is in line with our treatment of the single-chain properties.[9,10] The equilibrium free energy and structure of the interacting chains is then given by the extremum condition:

$$A_{12}(R) = \min_{\langle s_1^2\rangle,\langle s_2^2\rangle} A_{12}(R,\langle s_1^2\rangle,\langle s_2^2\rangle) \quad (16)$$

The minimum-energy radii of gyration vary with the interchain distance and are obviously equal by symmetry: $\langle s_1^2\rangle = \langle s_2^2\rangle = \langle s^2\rangle$. In the practical implementation of the optimization problem, we have made use of the DBRENT routine for one-dimensional minimization of ref 15, with the chain compression parameter q ($=q_1 = q_2$) as the only variable of the energy expression (7).

In the following, we shall also discuss a set of "frozen-chain" nonequilibrium calculations: instead of being optimized at each R, the chain radius of gyration remains everywhere equal to the single-chain value at the same temperature, or in other words to the equilibrium value for the chains at infinite distance. This perturbative approach is expected to work reasonably well near the Θ temperature. Being obtained by energy minimization, the equilibrium interaction energies are always lower (more negative) than the frozen-chain ones.

Numerical Results. Figures 2 and 3 contain plots of the chain interaction energies calculated for two different polymer systems (A and B, the same as in Figure 1). We present both the equilibrium and the frozen-chain results. The three temperatures chosen for the plots are $\tau B N^{1/2} = -0.20$, -0.30, and -0.60 for system A (Figure 2) and $\tau B N^{1/2} = -0.20$, -0.35, and -0.60 for system B (Figure 3): these are higher, approximately equal, and lower than the respective collapse temperatures (see Figure 1). Adoption of the reduced variable $R/\langle s^2\rangle_0^{1/2}$ for the x axis eliminates all the N-dependence from the plots, as can be seen by inspection of the energy expression.

Above the collapse temperature ,the equilibrium and the frozen-chain results are at least qualitatively similar (they are nearly identical in the case of system B, which

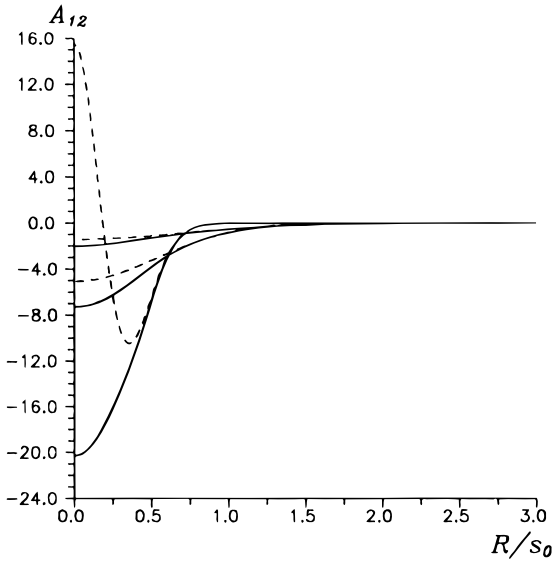

Figure 2. Equilibrium (continuous lines) and frozen-chain (dashed lines) interaction free energies between two A chains (see Figure 1) as a function of the normalized separation $R/\langle s^2\rangle_0^{1/2}$, at $\tau BN^{1/2} = -0.20$, -0.30, and -0.60 (the well depth increases with $|\tau|$).

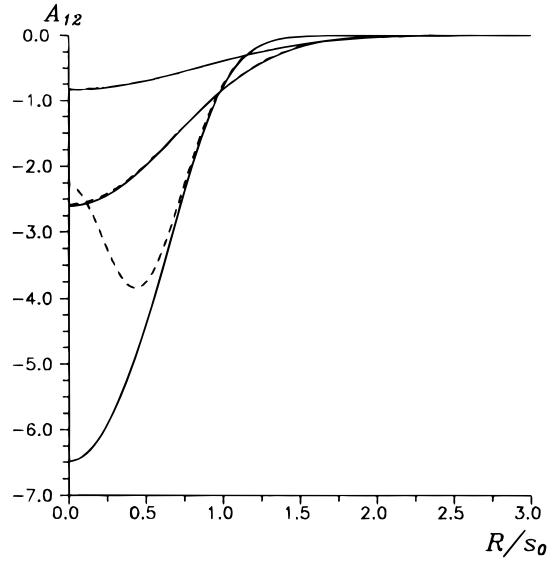

Figure 3. Equilibrium (continuous lines) and frozen-chain (dashed lines) interaction free energies between two B chains (see Figure 1) as a function of the normalized separation $R/\langle s^2\rangle_0^{1/2}$, at $\tau BN^{1/2} = -0.20$, -0.35, and -0.60 (the well depth increases with $|\tau|$).

is characterized by a larger K_1 parameter). The two interaction free energies are instead remarkably different at lower temperatures, when the isolated chains are in the collapsed state. Starting from large R values, the two chains are subject to a strong attraction until they begin to overlap appreciably. At shorter range the attraction becomes stronger and stronger in the equilibrium case, whereas it turns into repulsion in the other. This behavior is not unexpected and it can be rationalized by going back to the contact free energy expression, eqs 9−11. The two-body intermolecular attractions are effective at longer range than the three-body repulsions, since the former decay as $\exp\{-0.75R^2/\langle s^2\rangle\}$ and the latter as $\exp\{-R^2/\langle s^2\rangle\}$: hence the two-body interactions dominate the contact free energy whenever $R^2 > \langle s^2\rangle$. When $R^2 < \langle s^2\rangle$, instead, the three-body intermolecular repulsions may become dominant if the chain is in the collapsed state and its radius of gyration

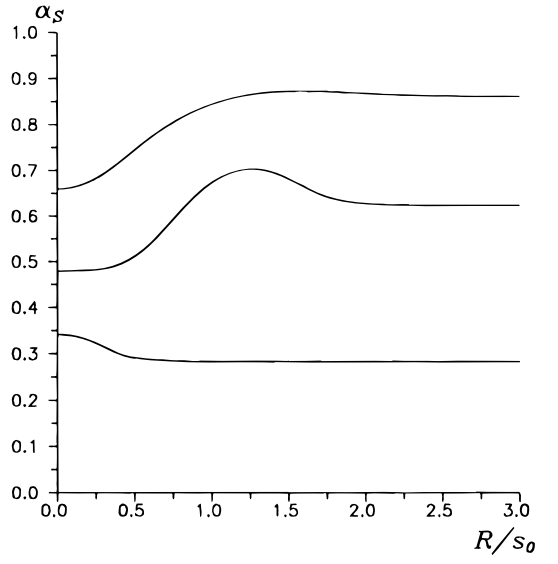

Figure 4. Equilibrium contraction ratios α_S for two A chains (see Figure 1) as a function of the normalized separation $R/\langle s^2\rangle_0^{1/2}$, at $\tau BN^{1/2} = -0.20$, -0.30, and -0.60 (from top to bottom).

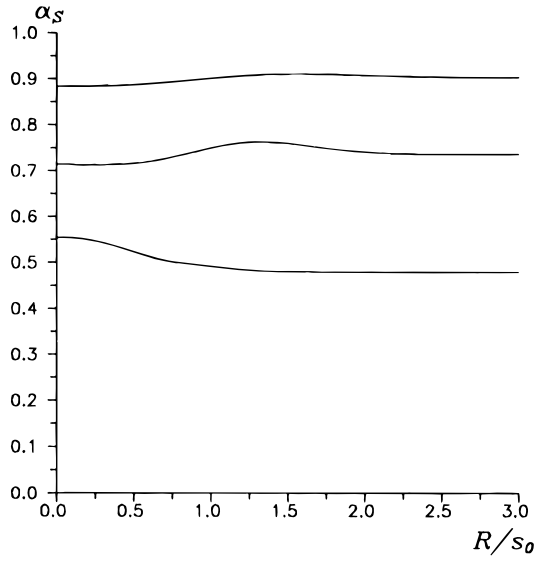

Figure 5. Equilibrium contraction ratios α_S for two B chains (see Figure 1) as a function of the normalized separation $R/\langle s^2\rangle_0^{1/2}$, at $\tau BN^{1/2} = -0.20$, -0.35, and -0.60 (from top to bottom).

is small enough ($\langle s^2\rangle \ll Nl^2$), as in the frozen-chain calculations.

Grosberg and Kuznetsov[8] released the constraint of spherical symmetry for the segment density of the individual chains. Despite this important difference, their free-energy curves are qualitatively similar to our equilibrium ones; however, it is difficult to perform a more precise quantitative comparison, due to the different nature of the theories. Tanaka's free-energy profiles[7], instead, are either everywhere attractive or everywhere repulsive (above and below the collapse temperature, respectively): the reason for this behavior can be traced to his assumption of a sharp density profile for the chains, which is probably too crude.

In Figures 4 and 5 we show plots of the equilibrium minimum-energy α_S as a function of the interchain distance, at the same temperatures. As in the case of the interaction energies, we see important qualitative changes as the temperature is lowered (this is particularly evident in the case of the small-K_1 A chains, in

Figure 4). Let us consider first the R-dependence of α_S above the collapse temperature: the size of the chains increases slightly until $R \simeq 1.5\langle s^2\rangle^{1/2}$ and then decreases at smaller distances. At $R = 0$, the radius of gyration of the two interacting chains is actually smaller than that of a single isolated chain: this is an important point, to which we return in the closing section. The driving force is provided by the two-body attractions: at long range these are maximized when the chains overlap by "stretching" toward each other, whereas at shorter range this is achieved when they collapse onto one another. These "oscillations" of α_S are even more pronounced at the collapse temperature: here the chain radius of gyration can be subject to large expansions or contractions under relatively small perturbations, such as a local temperature fluctuation or, in this particular case, the neighborhood of a second chain. Finally, below the collapse temperature the isolated chains are in a compact globular state and they expand once they start to overlap. Now the driving force behind this conformational change is represented by the three-body repulsions, which are substantially reduced by a modest increase of α_S.

Nonequilibrium Aspects. We have just seen that the equilibrium (variational) and the frozen-chain (perturbative) models can lead to radically different conclusions. These different schemes actually correspond to two opposite limits: that in which the intermolecular degree of freedom (R) has a much slower dynamics than the intramolecular ones ($\langle s_i^2\rangle$), and vice versa. So let us turn to a qualitative discussion of their reliability by comparing the "diffusion time" and the "conformational relaxation time" of the interacting chains.

During a time t the center of mass of a polymer molecule diffuses over a mean-square distance $\langle r^2\rangle$ given by

$$\langle r^2\rangle = 6Dt \tag{17}$$

In the Zimm limit with hydrodynamic interaction, the diffusion coefficient D is related to the chain hydrodynamic radius $\langle R_H\rangle$ and to the solvent viscosity η by

$$D = \frac{k_B T}{6\pi\eta\langle R_H\rangle} \tag{18}$$

We define the diffusion time τ_D as the time necessary for the chain to travel a distance of the order of magnitude of its size. We have

$$\tau_D \simeq \frac{\langle s^2\rangle}{D} \simeq \eta\langle s^2\rangle\langle R_H\rangle \tag{19}$$

In the globular state the chain monomers are tightly packed together, so that the volume of the collapsed polymer is proportional to N. This "space-filling" condition implies

$$\langle s^2\rangle \sim N^{2/3}; \qquad \langle R_H\rangle \sim N^{1/3} \tag{20}$$

so that

$$\tau_D \sim \eta N \tag{21}$$

As to the longest conformational relaxation time τ_C, in the Zimm limit this is given by (see for example ref 16)

$$\tau_C \sim \eta\langle s^2\rangle^{3/2} \tag{22}$$

Using eq 20, we then find

$$\tau_C \sim \eta N \tag{23}$$

Comparing eqs 21 and 23, we see that the time needed by the chains to adjust their configuration (τ_C) and the time needed to diffuse toward or away from each other (τ_D) show the same dependence on the polymer molecular mass and on the solvent viscosity, at least within the range of validity of the simple scaling relations given above. We conclude that neither the equilibrium nor the frozen-chain description of the encounter between two polymer molecules is fully satisfactory. Still, they do retain some of their interest. The equilibrium scheme clearly provides a lower bound for the chain interaction energy. It also seems reasonable to interpret the frozen-chain results as an upper bound to the interaction free energy, at least in the particular case of the encounter of two chains (the "dissociation" of two chains initially at $R = 0$ is yet another problem, from a nonequilibrium perspective): any kind of conformational relaxation, either full or only partial, must lead to a lowering of the free energy.

Having recognized the importance of nonequilibrium effects in poor-solvent macromolecular interactions, it is no longer possible to avoid at least a qualitative discussion of chain entanglements. Two collapsed chains with overlapping monomer densities have a high probability of being knotted together. The making and unmaking of these knots are complex, highly cooperative processes which are governed by reptation-like motions. Extrapolating to the present situation the well-known scaling relation for the corresponding relaxation time,[2−4] we have

$$\tau_K \sim \eta\frac{N^3}{N_e} \tag{24}$$

where N_e is the entanglement length of the polymer at hand. It has been demonstrated[17,18] that in a concentrated or semidilute solution this parameter has the following dependence on the polymer volume fraction:

$$N_e \sim \varphi^{-4/3} \tag{25}$$

Making one further extrapolation, we use this relation in eq 24 with φ as the segment density inside a single collapsed chain:

$$\tau_K \sim \eta N^3\left(\frac{N}{\langle S^2\rangle^{3/2}}\right)^{4/3} \sim \eta\frac{N^{7/3}}{\alpha_S{}^4} \tag{26}$$

The knotting time τ_K for long collapsed chains is thus guaranteed to be much longer than both τ_D and τ_C. Notice that chain collapse would also cause an increase of the viscosity η of the medium.

In conclusion, the encounter of two collapsed polymer molecules is characterized by at least two stages with distinct time scales (see also the discussion by Grosberg and Kuznetsov[6]): the initial, gradual conformational relaxation is followed by the formation of the interchain entanglements. Intermolecular knotting should be aided by the "segregation" of the free ends of the chains to the surface of the collapsed globules, which has been demonstrated in a previous theoretical study.[13] One possible complication to this simple picture is that a certain degree of intermolecular knotting might be a *prerequisite* for the compenetration of the chains, hence for a full conformational relaxation.

How does the presence of the interchain entaglements affect the significance of our equilibrium and frozen-chain results? In particular, can these still be considered a lower and an upper bound for the true interaction free energy? We believe the answer is yes. In the case of *ring* polymers there is a genuine topological constraint which prevents the two-chain system from visiting a certain subset of the configuration space (the catenane-like structures). This gives rise to a net repulsion between the chains, even when the contact free energy is zero.[19,20] In principle, this extra repulsive interaction could be accounted for within the present theory by some kind of *inter*molecular elastic free energy. The case of *linear* polymers is different: unless τ_K becomes comparable to or even longer than the "observation time", interchain entanglements do not give rise to an additional contribution to the interaction free energy.

III. Second Virial Coefficient

The virial expansion of the osmotic pressure of the dilute solution takes the following form:[2-4]

$$\frac{\pi}{k_B T} = c + \frac{M^2}{N_A} A_2 c^2 + \frac{M^3}{N_A{}^2} A_3 c^3 + \ldots \qquad (27)$$

where c is the number of chains per unit volume, M is the polymer molecular mass ($\propto N$), and N_A is Avogadro's number. The virial coefficients A_2, A_3, etc. are related to the chain interaction free energy introduced in the previous section. In particular, the second virial coefficient is proportional to the temperature-dependent cluster integral u:

$$A_2 = \frac{N_A}{M^2} u \qquad (28)$$

$$u = \frac{1}{2}\int d^3\mathbf{R}\,[1 - e^{-\Delta A_{12}(R)}] = 2\pi\int_0^\infty dR\, R^2[1 - e^{-\Delta A_{12}(R)}] \qquad (29)$$

$\Delta A_{12}(R)$ is the free-energy difference between two polymer chains at a distance R and the chains at infinite distance, at the same reduced temperature.

Figures 6 and 7 contain logarithmic plots of the second virial coefficient for systems A and B; the molecular-mass dependence is eliminated by the choice of $\tau BN^{1/2}$ and $A_2N^{1/2}$ for the coordinate axes. We present the equilibrium, the frozen-chain, and the mean-field results: for the purpose of the present discussion, we shall indicate them by $A_{2,eq}$, $A_{2,fc}$, and $A_{2,mf}$, respectively. The numerical differences between these quantities can be enormous: at $\tau BN^{1/2} = -0.6$, for example, the mean-field second virial coefficient of system A is 3 orders of magnitude smaller than $A_{2,fc}$ (in modulus), which in turn is smaller than $A_{2,eq}$ by another 3 orders of magnitude. The qualitative features of the curves are also very different. In proximity of the Θ temperature the behavior of $A_{2,eq}$ resembles that of $A_{2,mf}$, which is characterized by the linear law $A_2N^{1/2} \propto -|\tau|BN^{1/2}$. At the collapse temperature we find a minimum and then a limited increase of A_2 in the mean-field case, whereas in the equilibrium case we observe the crossover to an exponential temperature dependence ($A_2N^{1/2} \propto -\exp\{|\tau|BN^{1/2}\}$). The frozen-chain second virial coefficient is always bracketed by $A_{2,mf}$ and $A_{2,eq}$. In the case of the A chains it has an interesting oscillatory behavior below the collapse temperature. In particular, between

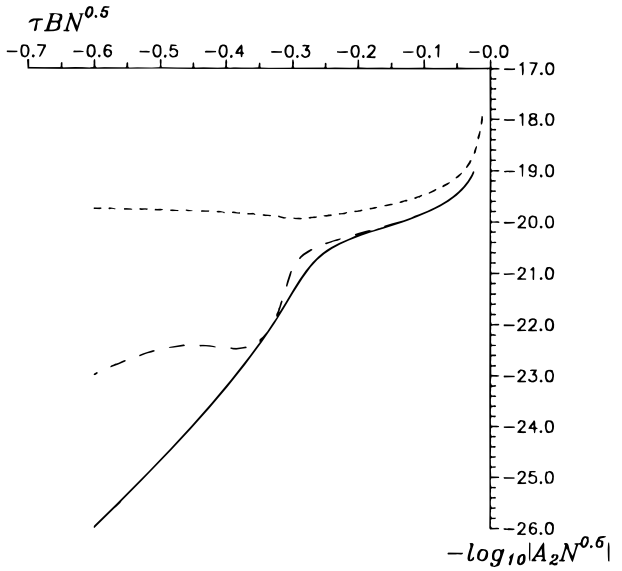

Figure 6. Equilibrium (continuous), frozen-chain (long-dashed), and mean-field (short-dashed) second virial coefficients of system A (see Figure 1); we plot $-\log_{10}|A_2N^{1/2}|$ as a function of $\tau BN^{1/2}$.

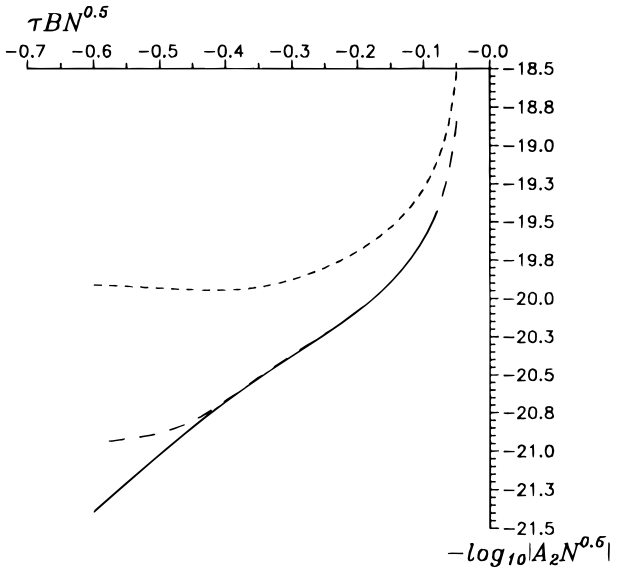

Figure 7. Equilibrium (continuous), frozen-chain (long-dashed), and mean-field (short-dashed) second virial coefficients of system B (see Figure 1); we plot $-\log_{10}|A_2N^{1/2}|$ as a function of $\tau BN^{1/2}$.

$\tau BN^{1/2} = -0.35$ and -0.45 it increases in a way similar to the mean-field coefficient.

The origin of the differences between $A_{2,eq}$ and $A_{2,fc}$ can readily be traced back to the shapes of the equilibrium and of the frozen-chain interaction potentials, which have been discussed in the previous section. Furthermore, it can be shown that there exists a simple relation between $A_{2,mf}$ and $A_{2,fc}$: the first is the leading term in the series expansion of the latter. If the conformation of the chains is R-independent and equal to that at infinite distance, we have (see eqs 9−11)

$$\Delta A_{12}(R) = \Delta A_2(R) + \Delta A_3(R) = -P\, e^{-pR^2} + Q e^{-qR^2} \qquad (30)$$

with

$$P = |\tau|BN^{1/2}(2^{-3/2})\left(\frac{\langle s^2\rangle}{Nl^2}\right)^{-3/2}; \qquad p = \frac{3}{4\langle s^2\rangle} \qquad (31)$$

$$Q = K_1(3^{-3/2})\left(\frac{\langle s^2\rangle}{Nl^2}\right)^{-3}; \qquad q = \frac{1}{\langle s^2\rangle} \tag{32}$$

Substitution into eq 29 followed by series expansion of the exponential and term-by-term integration leads to

$$\frac{u}{2\pi} = \int_0^\infty \mathrm{d}R\, R^2\left[1 - \sum_{k=0}^{\infty}\frac{(-1)^k}{k!}(\Delta A_2 + \Delta A_3)^k\right] \tag{33}$$

$$= \frac{\pi^{1/2}}{4}\sum_{k=1}^{\infty}\frac{(-1)^{k+1}}{k!}\sum_{j=0}^{k}\binom{k}{j}(-1)^j P^j Q^{k-j}[pj + q(k-j)]^{-3/2} \tag{34}$$

Using the definitions of P, p, Q, and q, we find that the first term in the series is

$$\left(\frac{u}{2\pi}\right)_{\mathrm{I}} = \left(\frac{\pi}{2\times 3^3}\right)^{1/2} N^2 l^3\left[\tau B + \frac{3^{3/2}K_1}{N^{1/2}\alpha_S{}^3}\right] \tag{35}$$

which should be compared with the mean-field result, eq 6. It could be shown that also the proportionality factors entering $A_{2,\mathrm{mf}}$ and the first term of $A_{2,\mathrm{fc}}$ are identical, provided the adjustable parameter D introduced in ref 1 is taken equal to $(^4/_3\pi)^{3/2}$ (there, we had tentatively set $D = {}^4/_3\pi$). Close to the Θ temperature chain interactions are weak and the $k \geq 2$ terms in the series can be neglected as a first approximation. This explains the substantial agreement between $A_{2,\mathrm{mf}}$, $A_{2,\mathrm{fc}}$, and $A_{2,\mathrm{eq}}$ above the collapse temperature and their dramatic disagreement below it.

Finally, in view of our discussion of the role of nonequilibrium effects in determining the shape of the chain interaction free energy, we remark that the true second virial coefficient should be bracketed by the equilibrium and the frozen-chain ones.

IV. Implications for the Polymer/Solvent Phase Diagram

The osmotic compressibility of the polymer solution diverges on the spinodal line.[2] Setting to zero the derivative of the virial expansion (eq 27) arrested to third order and solving the resulting equation, we find ($A_2 < 0$)

$$c_{\mathrm{sp}} \simeq -\frac{N_{\mathrm{A}}A_2}{3MA_3}\left[1 \pm \left(1 - \frac{3A_3}{MA_2{}^2}\right)^{1/2}\right] \tag{36}$$

The "+" and "−" signs correspond to the high- and the low-concentration branches of the spinodal, respectively. The latter becomes, when $A_3 \ll MA_2{}^2$,

$$c_{\mathrm{sp}} \simeq \frac{N_{\mathrm{A}}}{2M^2|A_2|} \tag{37}$$

As A_2 becomes more (less) negative, the spinodal shifts to lower (higher) concentrations. In view of the results from the previous section, we conclude that mean-field approximation provides a reasonable estimate of the position of the low-concentration branch of the spinodal above the collapse temperature. On the other hand, below the collapse temperature, it grossly overestimates the limit of metastability of the low-concentration homogeneous phase: the unphysical detour of the spinodal described in ref 1 and mentioned in the Introduction is an artifact of the mean-field approximation. Another important conclusion is that nonequilibrium effects, whose importance we have tried to estimate by means of the frozen-chain ansatz, can increase the limit of metastability of the dilute homogeneous phase by several orders of magnitude. Rather than being a simple "line", the spinodal is thus a very broad region on the temperature−concentration plane,[6] roughly delimited by the equilibrium and the frozen-chain curves.

Before closing this section, we provide some justification for the near-universality of the phase diagram for different polymer/solvent systems, which was observed in ref 1. In particular, we demonstrate a corresponding-states principle for the critical point. The high- and the low-concentration branches of the spinodal and the binodal merge at the critical point. Hence, it follows from eq 36 that this is determined by the two conditions

$$1 - \frac{3A_3}{MA_2{}^2} = 0 \tag{38}$$

$$c_{\mathrm{cr}} = -\frac{N_{\mathrm{A}}A_2}{3MA_3} \tag{39}$$

Let us introduce the polymer volume fraction φ and the chain length N:

$$N \propto M, \qquad \varphi = v_s Nc \propto K_1{}^{1/2}Nc \tag{40}$$

where v_s is the volume of one statistical segment, proportional to $K_1{}^{1/2}$ (see ref 11). Furthermore, we replace the second and the third virial coefficients with the leading terms of their mean-field expressions:

$$A_2 \propto (\tau - \tau_0)B \qquad A_3 \propto K_1 \tag{41}$$

where τ_0 has been defined in the Introduction as the temperature where A_2 vanishes (*i.e.*, the shifted Θ temperature). It follows immediately that eqs 38 and 39 can be cast in the form

$$(\tau_{\mathrm{cr}} - \tau_0)B\left(\frac{N}{K_1}\right)^{1/2} = \mathrm{const} \tag{42}$$

$$\varphi_{\mathrm{cr}}N^{1/2} = -\mathrm{const}' \times (\tau_{\mathrm{cr}} - \tau_0)B\left(\frac{N}{K_1}\right)^{1/2} = \mathrm{const}'' \tag{43}$$

Hence, the calculated critical point of a given polymer/solvent system always occurs at the same values of $(\tau - \tau_0)B(N/K_1)^{1/2}$ and $\varphi N^{1/2}$, whatever the parameters N, B, and K_1.

V. Concluding Remarks

In this paper, we have presented a simple computation of the interaction free energy between two polymer chains in a poor solvent ($T < \Theta$). There are many ways in which the accuracy of the calculation could be improved: by renouncing the simple Gaussian approximation for the chain segment density (eq 8) or by including medium-range "screened interactions"[9,10] in addition to the conventional two- and three-body contact energies, for example. However, even at the relatively simple level of theory adopted in this work, we have been able to highlight an important, essentially unsolved problem: the influence of the conformational relaxation dynamics and of the formation of temporary interchain entanglements on the polymer interaction free energy and the second virial coefficient. Our "equilibrium" and "frozen-chain" calculations demonstrate how large this effect can be, particularly below

the collapse temperature. The qualitative arguments presented at the end of section II for the relative magnitude of the diffusion ($\tau_D \sim \eta N$), conformational ($\tau_C \sim \eta N$), and knotting ($\tau_K \sim \eta N^{7/3}\alpha_S^{-4}$) relaxation times hint that the answer is not going to be simple, possibly requiring a combination of theory, experiment, and computer simulation.

The results of our numerical calculations are summarized by Figures 2−7. At the collapse temperature, we observe a switch in the equilibrium A_2 from a linear dependence on $\tau BN^{1/2}$—which is well described at a qualitative level by the mean-field coefficient (eq 6)—to an exponential dependence. In one case (Figure 6), the competition between the long-range attractive and the short-range repulsive parts of the frozen-chain interaction free energy causes an interesting oscillatory behavior of $A_{2,fc}$, just below the collapse temperature. In general, we have

$$A_{2,eq} < A_{2,fc} < A_{2,mf} \; (<0) \tag{44}$$

which in turn implies (see eq 37)

$$c_{sp,eq} < c_{sp,fc} < c_{sp,mf} \tag{45}$$

According to our qualitative arguments, $c_{sp,eq}$ and $c_{sp,fc}$ provide a lower and an upper bound for the position of the spinodal: rather than a "line", this should be seen as a broad region on the temperature−concentration plane (below the collapse temperature $c_{sp,eq}$ and $c_{sp,fc}$ can differ by orders of magnitude). On the other hand, our mean-field approach always overestimates the spinodal concentration.

The behavior of our mean-field A_2 has some similarity to that predicted theoretically by Tanaka,[7] with a somewhat unexpected upturn below the collapse temperature. In our case, the reason is to be found in the absence of any chain relaxation and the neglect of all high-order terms in the series expansion of A_2 (see section III); Tanaka, instead, computed the chain interaction free energy assuming a sharp density profile for the polymers. Whatever the reasons for it, this common result is likely to be incorrect. If some kind of upturn in A_2 was indeed present—as is suggested by the experimental findings of Nierlich *et al.*,[21] which however have been criticized in refs 22 and 23—it could only be justified by chain interactions accompanied by limited conformational relaxation (see the frozen-chain curve in Figure 6).

Finally, we briefly discuss the implications of our results for the interpretation of the light scattering experiments by Chu, Ying, and Grosberg on the kinetics of chain collapse and phase separation.[5] These authors essentially identified the onset of chain aggregation with the appearance in the solution of macromolecular clusters with a large hydrodynamic radius. However, they were also rather puzzled by the observation that the characteristic time for chain aggregation was about 2 orders of magnitude larger than what could be predicted on the basis of the polymer concentration and diffusion coefficient. They concluded that only ≃1% of the collisions between two chains effectively lead to their aggregation. However, there is a simpler, alternative explanation: substantial chain aggregation could have occurred long before the appearance of the large clusters. A cluster of ν chains ($\nu = 2, 3, ...$) is not necessarily ν times bigger than a single polymer molecule, the reason being that the two-body attractions are $\nu^{1/2}$ times stronger in the former than in the latter case. Indeed, our calculations show that above the collapse temperature a two-chain cluster can have a *smaller* radius of gyration than a single chain (compare α_S at $R = 0$ with α_S for $R \to \infty$ in Figure 4). In fact, the polydispersity index M_z/M_w of the small collapsed objects observed by Chu and co-workers increases from 1.48 immediately after quenching to 2.64 just before the appearance of the large aggregates, to be compared with $M_z/M_w = 1.02$ in Θ conditions. The fact that the clusters of two or three chains are actually compact, collapsed objects might also help to explain their inertia to aggregate further into larger structures (see our discussion of the nonequilibrium interaction free energy between two collapsed chains). We plan to investigate the structure and stability of these macromolecular clusters in a future paper, along the lines outlined in ref 1.

Acknowledgment. The authors thank Prof. Fabio Ganazzoli for useful and stimulating discussions and acknowledge financial support by the Italian Ministry for University and Research (MURST, 40% funds) and the Italian National Research Council (CNR, "Progetto Strategico Tecnologie Chimiche Innovative").

References and Notes

(1) Raos, G.; Allegra, G. *J. Chem. Phys.* **1996**, *104*, 1626.
(2) de Gennes, P.-G. *Scaling Concepts in Polymer Physics*; Cornell University Press: Ithaca, NY, 1979.
(3) Fujita, H. *Polymer Solutions*; Elsevier: Amsterdam, 1990.
(4) Grosberg, A. Yu.; Khokhlov, A. R. *Statistical Physics of Macromolecules*; AIP: New York, 1994.
(5) Chu, B.; Ying, Q.; Grosberg, A. Yu. *Macromolecules* **1995**, *28*, 180.
(6) Grosberg, A. Yu.; Kuznetsov, D. V. *Macromolecules* **1993**, *26*, 4249.
(7) Tanaka, F. *J. Chem. Phys.* **1985**, *82*, 4707.
(8) Grosberg, A. Yu.; Kuznetsov, D. V. *J. Phys. II (Fr.)* **1992**, *2*, 1327. Grosberg, A. Yu.; Kuznetsov, D. V. *Macromolecules* **1992**, *25*, 1991.
(9) Allegra, G.; Ganazzoli, F. *Adv. Chem. Phys.* **1989**, *75*, 265.
(10) Allegra, G.; Ganazzoli, F. *Prog. Polym. Sci.* **1991**, *16*, 463.
(11) Allegra, G.; Ganazzoli, F. *J. Chem. Phys.* **1985**, *83*, 397.
(12) Allegra, G.; Ganazzoli, F. *Gazz. Chim. Ital.* **1987**, *117*, 99.
(13) Allegra, G.; De Vitis, M.; Ganazzoli, F. *Makromol. Chem., Theory Simul.* **1993**, *2*, 829.
(14) Ganazzoli, F.; Allegra, G.; Colombo, E.; De Vitis, M. *Makromol. Chem., Theory Simul.* **1992**, *1*, 299.
(15) Press, W. H.; Flannery, B. P.; Teukolsky, S. A.; Vetterling, W. T. *Numerical Recipes* (Fortran version); Cambridge University Press: Cambridge, 1989.
(16) Ganazzoli, F.; Forni, A. *Macromolecules* **1995**, *28*, 7950.
(17) Colby, R. H.; Rubinstein, M. *Macromolecules* **1990**, *23*, 2753.
(18) Richter, D.; Farago, B.; Butera, R.; Fetters, L. J.; Huang, J. S.; Ewen, B. *Macromolecules* **1993**, *26*, 795.
(19) Iwata, K. *Macromolecules* **1985**, *18*, 115.
(20) Tanaka, F. *J. Chem. Phys.* **1987**, *87*, 4201.
(21) Nierlich, M.; Cotton, J. P.; Farnoux, B. *J. Chem. Phys.* **1978**, *69*, 1379.
(22) Sun, S. T.; Nishio, I.; Swislow, G.; Tanaka, T. *J. Chem. Phys.* **1980**, *73*, 5971.
(23) Park, I. H.; Wang, Q.-W.; Chu, B. *Macromolecules* **1987**, *20*, 1965.

MA960503I